

1

2 **ASPHALT SURFACE DAMAGE DUE TO COMBINED ACTION OF WATER AND**
3 **DYNAMIC LOADING**

4 Fauzia Saeed^{*1}; Mujib Rahman²; Denis Chamberlain³, Phil Collins⁴

5
6 **ABSTRACT**

7 Water ingress causes significant deterioration in asphalt surfaces. In this study, a novel laboratory test method has been
8 developed to study the combined interaction of water-tire-pavement on the performance of four open graded and two
9 gap-graded asphalt mixtures produced with 6mm, 10mm and 14mm nominal maximum aggregate size. A dynamic
10 load with a fixed frequency was applied while the surface was submerged with up to 2mm water. The test continued
11 until the specimens showed significant failures. Compared to dry condition testing, despite relatively good rutting
12 performance, the appearance of surface crack was approximately seven times faster in open-graded mixtures tested in
13 wet conditions, indicating accelerated deterioration due to the presence of water. The gap graded mixtures, on the
14 other hand, showed better cracking resistance but inferior rutting performance. Finally, for same mixture tested in wet
15 condition, mixtures with larger aggregate size showed more overall deterioration than mixtures with smaller size
16 aggregates. The method has good potential to be implemented as a screening test for different types of mixes to study
17 their water susceptibility due to combined action of tire-water-pavement.

18

19 Key words: asphalt pavement, fatigue cracking, rutting, water damage.

20

*Corresponding author, PhD candidate, Department of Civil and Environmental Engineering, Brunel University London UB8 3PH
Fauzia.Saeed@brunel.ac.uk

¹ Department of Civil and Environmental Engineering, College of Engineering, Omer Al-Mukhtar University, Libya

² Senior Lecturer, Department of Civil and Environmental Engineering, Brunel University London UB8 3PH
mujib.rahman@brunel.ac.uk

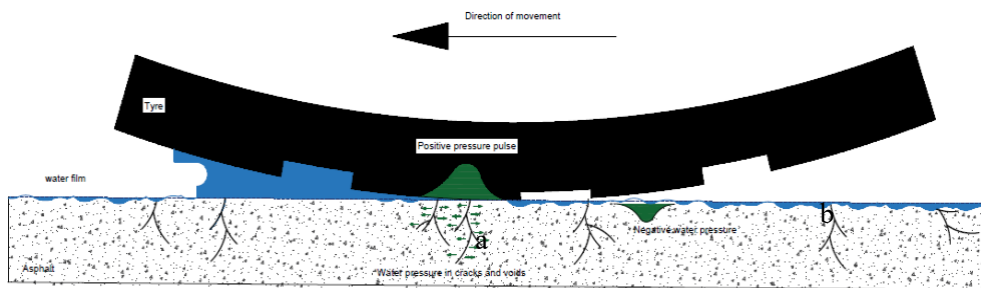
³ Visiting Professor, Department of Civil and Environmental Engineering, Brunel University London UB8 3PH
denis.chamberlain@brunel.ac.uk

⁴ Senior Lecturer, Department of Civil and Environmental Engineering, Brunel University London UB8 3PH
philip.collins@brunel.ac.uk

21 INTRODUCTION

22 Flexible pavements are designed to withstand mechanical and functional degradation due to traffic and environmental
23 loading. [1-8]. Premature failure leads to reduce service life, compromises the safe operation of traffic, and increases
24 maintenance and rehabilitation cost. In recent years, there are significant public concerns due to the rapid increase in
25 the number of damages, namely potholes, in the asphalt surfaces (9). These localized failed areas reduce the ride
26 quality and potentially create a dangerous driving condition. A survey by Asphalt Industry Alliances in 2018 revealed
27 that nearly one-third of the local authorities in the United Kingdom felt that the roads had to be shut down due to safety
28 hazards [10].

29 Although it is well known that water ingress in pavement causes significant deterioration, the mechanism is
30 not yet fully understood, especially its impact on the surface damage [10]. There are two sources of water/moisture in
31 asphalt pavement, internal and external. Inadequate drying of aggregate used in the mixes can be one common internal
32 sources of moisture [11, 12]. An external source of water can come from three different ways; water is entering the
33 pavement from surfaces because of poor drainage, poor construction [compaction] or mixture design having high air
34 voids content and so more permeability. Water can also enter in pavements from the sides because of poorly
35 constructed shoulders, poor side drainage and water beneath the subgrade because of the high water table and poor
36 drainage characteristics of base and sub-base material [13]. It is believed that the water on the surface or water build
37 up in the pavement structure exacerbates surface damage with moving traffic, which may eventually result in
38 pavement surface layer spalling or loosening, leading to localized as well as structural damage [14-17]. A conceptual
39 illustration of water movement and subsequent tire-pavement interaction is shown in Figure 2. When external water is
40 present, there are two ways it may influence an asphalt mixture: (a) a flow field through pore structures, and (b) static
41 water near the surface.



42
43 **Figure 1 Conceptual illustration of tire-water-pavement interaction**

44 If a flow field is present, water may wash away the mastic, weaken the binder, and cause a decrease in the cohesion and
45 mixture stiffness, incurring damage to the road. The magnitude of the flow field and water pressure within the asphalt
46 road is also dependent on tire characteristics (tire pressure, tread shape, depth, and patterns), traffic
47 characteristics[magnitude, speed] as well as mixture configurations such as size and gradation of aggregate, void
48 contents and level of compaction. The influences of these parameters on the pore pressure in pavement surface are
49 under investigation in a parallel study by the authors [18]. Static water, on the other hand, gradually penetrates the
50 asphalt and aggregate interface and thus easily causes a reduction of adhesion between asphalt binder and aggregate
51 surface [15, 19]. Zhang et al. 2014 stated that high tensile localized stresses near the edges of a compressed air void
52 could lead to the growth of the crack in an asphalt mixture under external compressive loads.

53
54 Besides, researchers examined the thick overlay and stated that cracks start at a surface and propagate downward. The
55 number of cracks decreased with the increase in the strength and thickness of the asphalt pavement [20] [21]. There are
56 two main directions for the compressive cracks that govern the rupture of the asphalt pavement in compression: the
57 first is the splitting cracks or diagonal cracks based on the stiffness and initial air void contents of the asphalt mixtures.
58 Usually, a stiffer asphalt mixture with low air void content tends to be split whereas a softer asphalt mixture with high
59 air void content tends to have a diagonal crack in the compression load [22]. A comparative investigation was
60 conducted [23] on three different HMA (Hot Mix Asphalt), with the maximum nominal size of 12.5, 19 and 25 mm. It
61 was noted that the larger gradation had, the lower fatigue life, which means that the gradation containing 12.5 mm
62 maximum nominal size had the highest fatigue life followed by the gradation including 19 and 25 mm maximum
63 nominal sizes. The influence of the aggregate gradation on the fatigue behaviour is more significant than the impact of
64 the binder content [24]. It was observed that the mixture with the larger aggregate gradation and higher asphalt content
65 exhibited lower fatigue life, while the larger aggregate gradation is a positive point for the rutting performance of the
66 asphalt pavement [20]. The simulation of the crack that is induced by dynamic loading is reasonable and applicable

67 when it is compared with a range of the previous fatigue tests because, instead of a static load, the cyclic dynamic load
68 is applied to the specimens; thus, it saves time and cost . Myers et al., [1998] who employed a computer model stated
69 that tensile stresses under the treads of the tire—not the tire edges—were the main reason for the cracks. Furthermore,
70 the wide-base tires caused the highest tensile stresses. They observed that the tensile stresses dissipate rapidly with
71 depth, suggesting that this possibly is the cause for the cracks to stop growing; on the other hand, they pointed out that
72 the issue required further study [25]. Tire forces measurement display non-uniform contact pressures [26]. Moreover,
73 they illustrated that the tire contact pressure is directly related to the wheel load magnitude. Additionally, the
74 modelling demonstrated that high shear stresses and strains happen under truck tires.

75 **PROBLEM STATEMENT**

76 Studies on water-related distresses are predominantly manifested towards material degradation of laboratory
77 fabricated specimens by evaluating the reduction of mechanical properties after several moisture conditionings cycles
78 and determining the loss of adhesion and cohesion of the mixture matrix [1]. However, the interaction of
79 tire-water-pavement happens simultaneously, and it is essential to study their combined impact on the overall
80 performance of the asphalt surface. In addition, previous research into pavement performance prediction has paid little
81 serious attention to surface-originating damage, despite a recent TRL (Transport Research Laboratory) study
82 highlighting that surface cracking and ravelling were the dominant failure modes on major roads in the UK [27]. In
83 addition, there is no standard test method to evaluate asphalt surface performance due to combined action of water and
84 loading. A significant knowledge gap, therefore, exists which this project aims to address.

86 **RESEARCH OBJECTIVES**

87 The primary aim of this research is to evaluate the performance of different asphalt surfaces subjected to concurrent
88 flooding and repeated loading. This paper presents a novel laboratory test set-up to represent the combined action of
89 water and traffic loading. Three widely used asphalt surfaces; a gap graded mixture such as hot rolled asphalt
90 (HRA) and two open-graded mixtures, such as stone mastic asphalt (SMA0) and porous asphalt (PA) were tested under
91 a dynamic load in both dry condition and, while submerged in a shallow water. The impact of voids contents and size
92 of aggregates are also studied. This paper covers two aspects of the study. The first section describes the test set-up and
93 experimental programmes, while the second part presents the test results concerning surface cracking, permanent
94 deformation and visual distress such as ravelling. All results are compared with the results from dry condition testing.

95 **EXPERIMENTAL PROGRAMME**

96 **Mixture design and sample preparation**

97 Mixtures were designed using relevant BS EN standards [28]. The gradation of each mixture, together with its
98 reference to standard is given in Figure 2. The 6mm HRA and 10mm Porous asphalts were not tested, as they are not
99 widely used surfacing type.

100 The aggregates, bitumen and filler were mixed according to BS EN 12697-35: 2004 [28]. The mixture was then poured
101 into a preheated custom build split 200mm×200mm×50mm steel mould at 140°C and then compacted using a
102 handheld vibrating compactor to the desired slab thickness to achieve the required air void contents. The direct force
103 applied to the slab, and the vibration frequency was chosen before compaction and therefore, can be assumed as
104 constant throughout the compaction process. Previous research has demonstrated that the procedure could be used to
105 simulate field compaction [29].

106 Six identical specimens were produced for each mixture combination to evaluate test repeatability and the sufficient
107 number of specimens for statistical analysis. The specimen was kept inside the mould for 24 hours at room temperature
108 and then extracted and placed inside a similar size prefabricated slot in a 305mm × 305mm × 80mm size C40 concrete
109 slab. The purpose of slotted concrete slabs was to provide confinement and an impermeable base, so that water is
110 stored in the asphalt surface, i.e. no water percolate in the lower layer. This is to simulate the worst-case scenario in the
111 asphalt pavement. This arrangement was found useful to minimize the influence of lower asphalt layer on the
112 performance of asphalt surface. A picture of the compaction device, compacted specimens and the specimen inside the
113 slotted section in the concrete slab is shown in Figure 3.

114
115
116
117
118
119
120
121

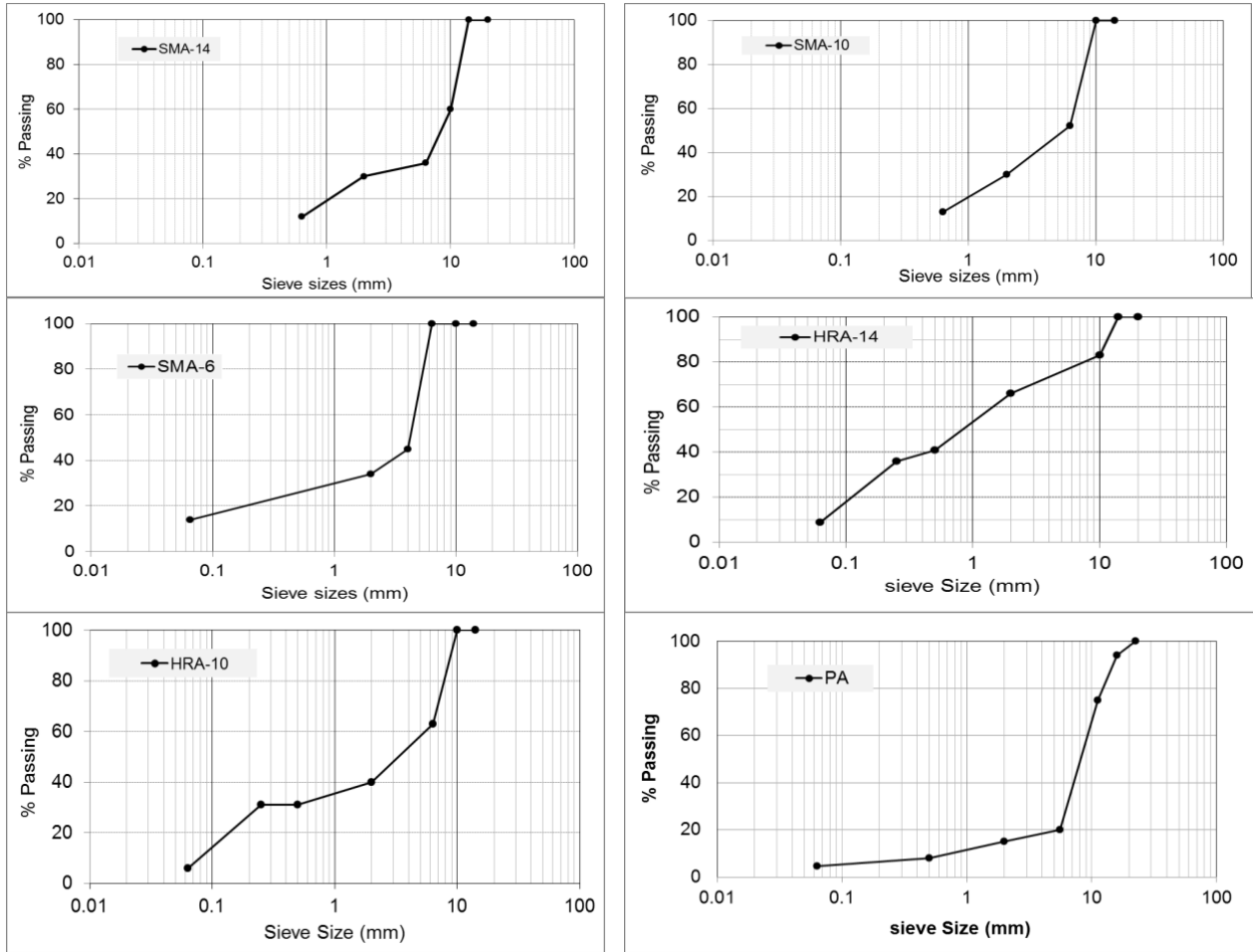
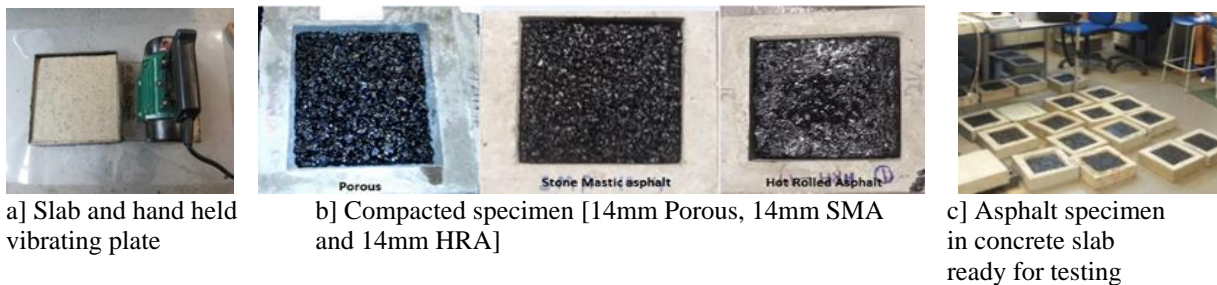


FIGURE 2 Gradatio curves for mixture types



123 a) Slab and hand held vibrating plate

b) Compacted specimen [14mm Porous, 14mm SMA and 14mm HRA]

c) Asphalt specimen in concrete slab ready for testing

124 FIGURE 3 Compaction device and compacted specimens

125 **Properties of compacted specimens**

126 The dimensions of each specimen were measured and then tested for bulk density as detailed in BS EN 12697-6:
 127 2003[30]. The actual percentage of air voids of each test specimen calculated according to BS EN 12697-8: 2003[31].
 128 The target void content was 8-13% for the SMA [Stone Mastic Asphalt]; it was 4-6% for the HRA [Hot Rolled
 129 Asphalt] and >16% for the PA [Porous Asphalt]. The actual VC [void contents] and VMA [voids in mineral
 130 aggregates] are also calculated. The sample properties are given in Table 2. It can be seen that all mixtures showed
 131 representative VC and VMA as required by the standard.

132
 133

134 **TABLE 2 Sample properties**

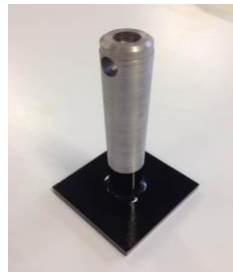
Mixture Type	Aggregate properties			No of sample	Specimen Size [mm ³]	Void contents [%]				VMA [%]
	Nominal maximum size [mm]	Type	Filler			Max	Min	Std	AVG	
HRA	10	Granite	Granite	6	200×200×50	7.81	5.97	0.736	6.5	18.86
	14	Granite	Granite	6	200×200×50	8.00	5.20	1.017	6.31	19.28
SMA	6	Granite	Granite	6	200×200×50	12.78	8.97	1.421	10.59	15.89
	10	Granite	Granite	6	200×200×50	13.63	10.36	1.371	11.87	15.02
	14	Granite	Granite	6	200×200×50	1.50	10.33	1.024	11.13	14.13
PA	14	Granite	Granite	6	200×200×50	20.89	18.00	1.315	19.51	11.19

135
 136 VMA is essential from the standpoint of durability. Mixture with high VMA will promote binder hardening that could
 137 cause of asphalt surface cracking and deterioration. Contrary mixtures with inadequate VMA will be tended to suffer
 138 from bleeding that explains shorter service life than expected of porous asphalt as compared to the dense mixture [33].
 139 VMA in SMA mixture has a negative relation with the nominal size of aggregate (NMAS)[34].

140 **Test-set-up**

141 The experimental programme consisted of designing a new 100mm² steel loading plate [Figure 4a] and then attached
 142 to an INSTRON machine capable of applying dynamic loading. The steel plate is adaptable to attach a 12mm thick
 143 rubber sheet with 8mm square tread (Figure 4b). The selection of tread patterns was adopted from earlier research by
 144 authors on the influence of tire tread shape and pattern on water pressure in the pavement. The results showed that
 145 water pressure at the bottom of surface increases when high-frequency loading combined with square types of tread
 146 pattern where water get trapped inside the square tread [18,35, 36,37].

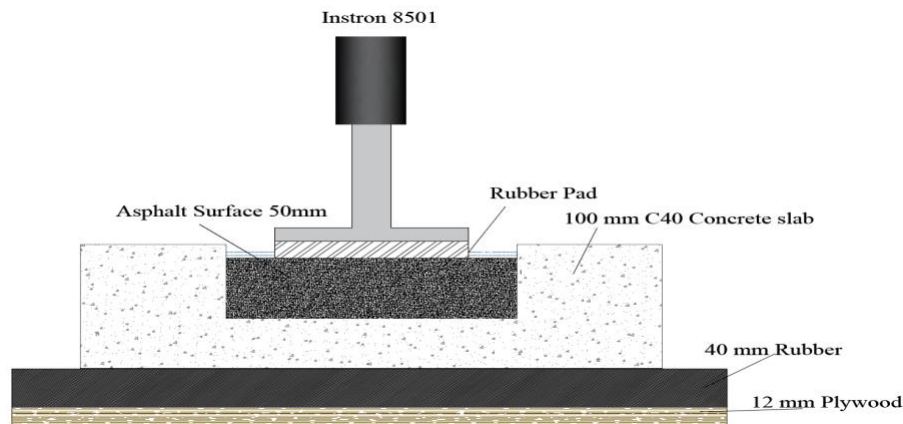
147
 148



(a) 100mm X 100mm loading plate



(b) Rubber pad representing tread shape



(c) Dynamic loading test set up

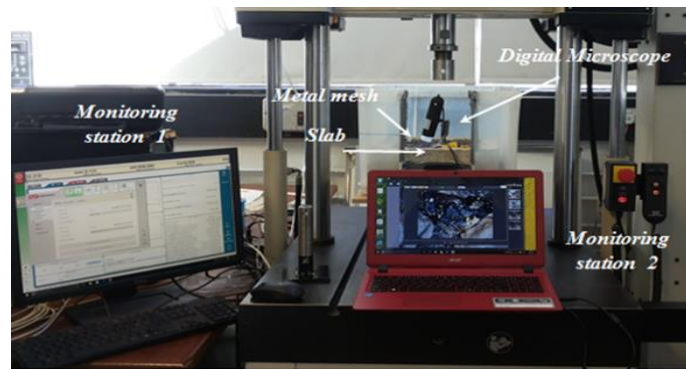
FIGURE 4 Schematic diagram of simulated pavement structure.

149
 150
 151
 152
 153
 154

155 Figure 4c represents a schematic diagram of simulated pavement structure. As mentioned earlier, an eighty mm
 156 concrete slab base was used to simulate lower asphalt layers and a 40mm rubber pad was to represent the pavement
 157 foundation.

158
 159 A 5kN sinusoidal compression load at a frequency 5Hz was applied. First, the loading plate was lowered on the surface
 160 with pre-load 0.5kN to ensure load plate is firmly placed on the surface, and then 4.5kN load was applied continuously
 161 until the test was completed, i.e. the magnitude of maximum and minimum load was 4.5kN and 0.5kN respectively.
 162 The selection of load magnitude and load frequency was based on the previous research on water pressure
 163 measurement by the authors [18]. The set-up and test specifications are given in Figure 5 and in Table 3. For each
 164 mixture type, three specimens were tested in dry condition and three in wet condition. The surface was submerged
 165 with 1-2mm water and this depth was kept constant during the duration of test by constant feeding of water. Specimens
 166 tested in wet condition went through overnight conditioning in water at room temperature to ensure saturation prior to
 167 testing. The samples were exposed to a total 20,000 to 40,000 load cycles. All 6mm and 10mm HRA and SMA
 168 mixtures were tested for 20,000 cycles while testing for all 14mm HRA, SMA and Porous asphalt mixtures were
 169 ceased after 40,000 cycles due to excessive amount of failure.

170
 171



172
 173 **FIGURE 5 Test set-up**

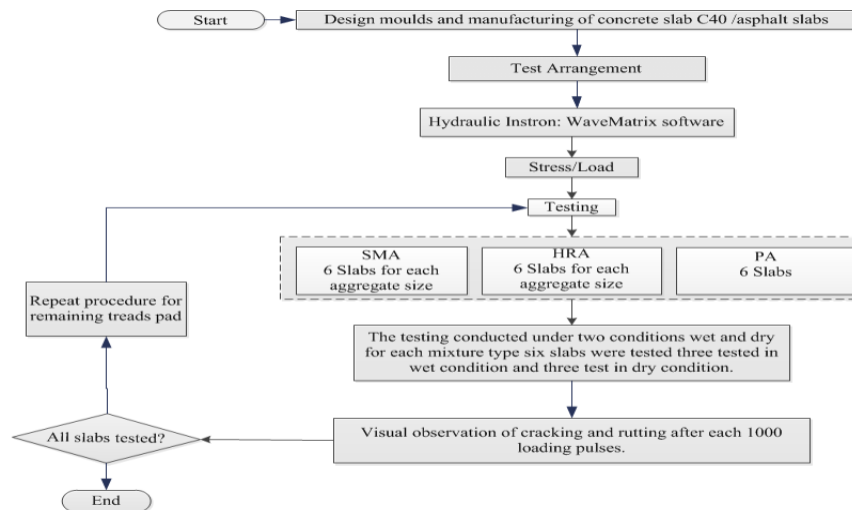
174
 175
 176

TABLE 3 Testing specifications

Asphalt type and tests conditions	Load [kN]	No of Sample	Frequency [Hz]	Water depth [mm]	Load cycles	Test temperature $\pm 1^{\circ}\text{C}$	Tread depth [mm]
HRA10-D	5	3	5	1-2	20,000	20	8
HRA10-W	5	3	5	1-2	20,000	20	8
HRA14-D	5	3	5	1-2	40,000	20	8
HRA14-W	5	3	5	1-2	40,000	20	8
SMA6-D	5	3	5	1-2	20,000	20	8
SMA6-W	5	3	5	1-2	20,000	20	8
SMA10-D	5	3	5	1-2	20,000	20	8
SMA10-W	5	3	5	1-2	20,000	20	8
SMA14-D	5	3	5	1-2	40,000	20	8
SMA14-W	5	3	5	1-2	40,000	20	8
PA14-D	5	3	5	1-2	40,000	20	8
PA14-W	5	3	5	1-2	40,000	20	8

177
 178
 179

For better understanding, a flow chart for testing programme is presented in Figure 6



180
181

FIGURE 6 A flowchart of the testing programme.

182 **Distress measurements**

183 After each determined number of cycles, the resulting vertical deformation of the asphalt lab and the length of the cracks appearing on the surface were measured. The procedure to measure distresses is given in following sections.

185 **Visual observation**

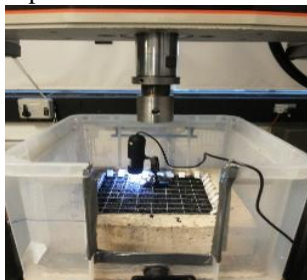
186 The visual observation [accumulative cycles, individual crack length, rutting and comments] was recorded in a standard survey sheet based on distress identification manual for the long-term pavement performance program [37].
187 Photographic evidences were recorded by camera and microscope. A mesh plate and ruler were used to measure pattern and length of cracks [mm], depth of rutting [mm]. Other distress such as corner cracking, loss of particles after every 1000 cycles were also recorded.

191 **Crack measurement**

192 After every 1000 cycles, the load device was lifted so that the slab surface was visible. Then, the sample was evaluated, and the presence of cracking was measured. Once a crack initiated, a picture was taken using the microscope with 400× magnifications to measure the length of the crack using the image processing software. The length of the crack was recorded, marked and accumulated to get a total length of the crack for subsequent 1000 cycles. Similar procedure was followed in wet condition testing; accept after lifting the load device, the asphalt surface was dried by a blotting paper prior taking any measurement. The set-up and marked specimens are shown in Figures 6a and 6b.

199 **Rutting measurement**

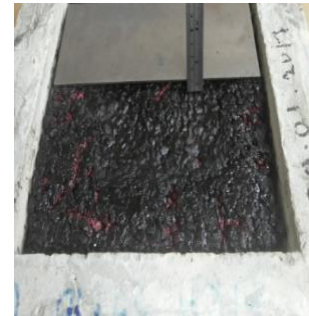
200 The rutting of the asphalt slab surface was measured after each 1000 load cycles by placing the straight plate in a plane perpendicular to the load direction, and the bottom surface of the plate was parallel to the longitudinal slope of the asphalt slab surface. The measurement set-up is shown in Figure 6c.



a) microscopic measurement of cracks



b) marked slab



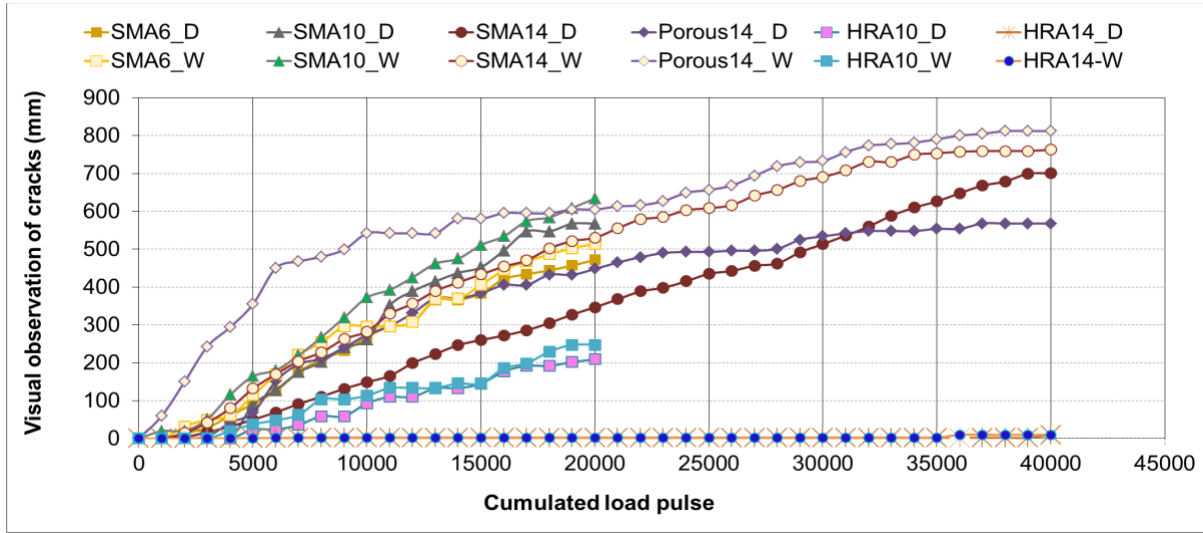
c) deformation measurement

203

FIGURE 8 Observations of distress

204 **RESULTS AND ANALYSIS**

205 The average cumulative length of cracking and cumulative rutting for each mixture tested in dry and in wet condition
 206 is shown in Figures 9 and 10 respectively.
 207



208 **FIGURE 9 Average cumulative cracking for all mixtures tested in the dry and wet conditions**

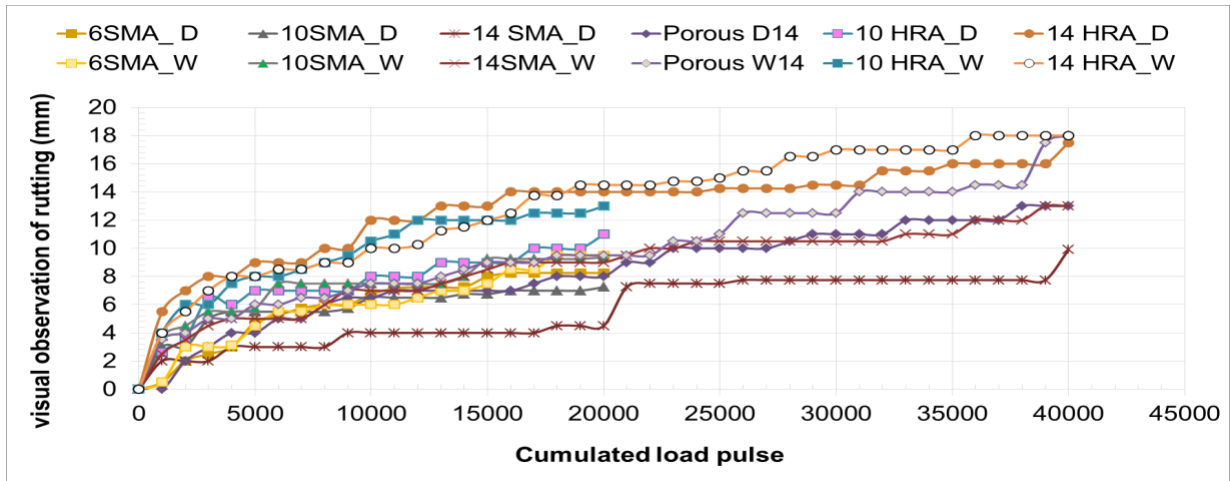


FIGURE 10 Maximum permanent deformations

209 The standard deviation of each test at both wet and dry conditions are given in the following Table 4. It can be seen that
 210 there are variations in the cracking results for all mixtures, but the rutting results are relatively consistent between
 211 samples.
 212

213 **TABLE 4 The standard deviation of wet and dry conditions at the end of tests.**

Standard Deviation	Asphalt Mixture					
	SMA-6	SMA-10	SMA-14	HRA-10	HRA-14	PA
Cracking	30.05	47.02	44.28	27.22	2.83	172.53
Rutting	0.88	1.50	2.19	1.41	.35	3.54

214

215 It is evident from the test results presented in Figures 9 and 10 that the presence of water significantly accelerates
 216 surface cracking. The affect is more severe in 14mm porous asphalt, then respectively to 14, 10 and 6 SMA and least in
 217 10mm and 14mm HRA. The cracking was almost negligible in 14mm HRA.

218 As with the cracking results, irrespective of mixture types, the resistance to permanent deformation of the asphalt
 219 mixtures decreases with the presence of water. Both 10mm and 14mm HRA mixtures showed significant rutting after
 220 40,000 load cycles compared to any SMA or Porous asphalts. The mechanical properties of the HRA come from the
 221 cohesion of the binder within the fine aggregates so that HRA can be less resistant to internal movement, but it can be
 222 better in fatigue crack resistant.

223 In addition to rutting and cracking, some ravelling was also observed in all SMA and Porous asphalt mixtures after
 224 the wet test, but it was negligible in mixtures tested in dry condition. Very little material loss was observed in both
 225 HRA mixtures. It is important to note that the damage pattern and relative quantity of damage were similar in all
 226 three-specimens tested for each mixture in dry condition and three specimens tested in wet condition.

227

228 **DISCUSSIONS**

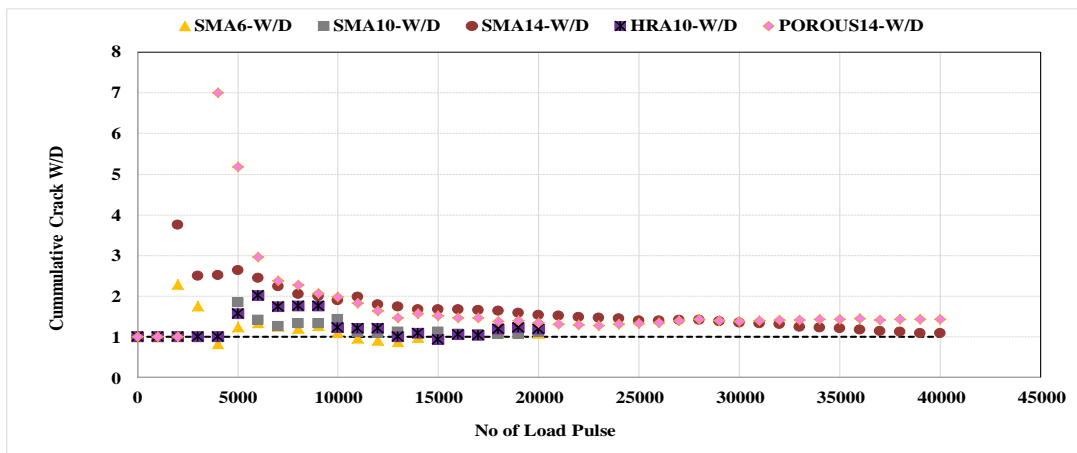
229 **Influence of combined action of water and loading**

230 Concerning dry versus wet crack severity, the relative effect is shown in Figure 11, where the ratio between wet
 231 and dry cracking at each load pulse is presented and in Table 4, the number of load cycles for 1st cracks and
 232 propagation of cracks and their severity level in light with FHWA [2003] is presented. Classification for alligator
 233 cracking is given [38]. FHWA crack severity classification is based on measurement of crack in 300mm on longest
 234 and recorded in the square meter. This was scaled down to 70 mm to 100mm with a few connecting cracks in tested
 235 200mm² for low severity [L], 100mm to 150mm with interconnected cracks for moderate severity [M], greater than
 236 150mm interconnected cracks forming a complete pattern and pieces move with loading, high severity [H][38].

237

238 The presence of water in the same asphalt mixture, compacted in the same manner, leads to increased cracking in the
 239 asphalt. It is has appeared that the gradation has more influence on both cracking than the actual size of aggregate. For
 240 example, 6mm and 14mm SMA appear to have inferiors cracking resistance than 10mm SMA. Besides, the crack
 241 appearance on the wet porous surface is more than seven-times in the dry state at the same load cycle. On the other
 242 hand, it is approximately twice as fast in SMA mixtures. Water on the surface has minimum impact on the HRA
 243 surface cracking. This is primarily due to the gradation of the mixtures, as Porous and SMA mixtures contain
 244 aggregate contact whereas HRA has more binder in the mix making it resilient to crack. It is likely that water or
 245 moisture entrapped within the asphalt mixtures can lead to the pore pressure build-up due to the repeated traffic loads.
 246 The continuation of the process of the pore pressure build-up ultimately leads to the degradation of the adhesive bond
 247 strength of the mastic [bitumen-filler] and that of the aggregates resulting in the growth of micro-cracks in the asphalt
 248 mixtures. It is also interesting to note that that air voids do not seem to influence wet condition performance. For
 249 example, despite similar void contents in SMA 14 [12.5% voids] and SMA 10 [13.63% voids], SMA 10 was not very
 250 sensitive to wet conditions as it was in SMA14. It has appeared that aggregate nominal size may have an impact on wet
 251 condition performance.

252



253

254

255

FIGURE 11 Comparison between wet and dry cracking

256

TABLE 5 Impact of combined action of surface water and loading on surface cracking

257

Mixture ID	Number of load pulse and corresponding cumulative length of crack			
	1 st	70 mm to 100mm with a few connecting cracks	100mm to 150mm with interconnected cracks	> 150mm interconnected cracking forming a complete pattern and pieces move with loading
HRA10_D	4042	9320	10236	14664
HRA10_W	3050	7180	7820	15096
HRA14_D	6000	40,000*	-	-
HRA14_W	5000	40,000*	-	-
SMA6_D	1070	4350	5120	6420
SMA6_W	1030	4313	4780	5640
SMA10_D	4012	4785	5192	6448
SMA10_W	50	3290	3712	4576
SMA14_D	1250	6037	7360	10001
SMA14_W	1065	3732	4344	5420
PA14_D	2160	5025	5400	5960
PA14_W	17	1110	1432	2000

258

259

* The cracks length in HRA14 mixture was 10 mm for both cases with the number of load pulse 40,000.

260

261

262

263

264

265

266

267

TABLE 6 Maximum rutting

Mixture ID	@ 20,000 load cycles		@40,000load cycles	
	Measured rutting [mm]	DMRB criteria Low Severity <6mm 6mm< Medium <11mm High severity>11mm	Measured rutting [mm]	DMRB criteria Low Severity <6mm 6mm< Medium <11mm High severity>11mm
HRA10_D	11.4	H	-	-
HRA10_W	13.2	H	-	-
HRA14_D	14.3	H	14.5	H
HRA14_W	17.5	H	18	H
SMA6_D	8.3	M	-	-
SMA6_W	9.5	M	-	-
SMA10_D	7.5	M	-	-
SMA10_W	9.4	M	-	-
SMA14_D	4.5	M	9.9	M
SMA14_W	9.0	M	13	H
PA14_D	8.2	M	13	H
PA14_W	9.5	M	18	H

268

269

Influence of aggregate size

270

271

272

273

274

The size of aggregate in the mixture appears to improve rutting performance in the dry condition, although this advantage diminishes when the mixture is exposed to the combined action of water and loading. For example, maximum rutting after 20,000 load cycles for dry tested 6mm SMA was 8.3mm, 10mm SMA was 7.5mm, and 14mm SMA mixtures was only 4.5mm. The corresponding rutting for all three mixtures tested in wet conditions was approximately 9mm. On the other hand, despite better cracking resistance, the rutting performance for 14mm HRA

275 was marginally inferior to 10mm HRA in both dry and in wet conditions. This is probably due to slightly more binder
276 content in the mixture in 14mm HRA [refer to Table 1]. Although not conclusive, another interesting point to note that,
277 the rutting performance after 40,000 load pulses, 14mm SMA outperformed 14mm Porous and 14mm HRA mixtures
278 in both dry and wet conditions. It appears that the gradation of the mixtures is has some influence than the size of
279 aggregate.

280 **Influence of mixture volumetric**

281 Mixture volumetric also have influence on the resistance to water. Both PA [VC ~ 19%, VMA ~14%] and SMA [VC
282 ~12% and VMA ~15%] failed significantly faster than HRA, with relatively low VC and high VMA [VC~ 6%, VMA~
283 19%]. The phenomenon is governed by the physicochemical interactions between bitumen and aggregates. Due to
284 their interactions, both chemically and physically, PA and SMA with thin film thickness appears to break up faster by
285 pumping of water in the larger interconnected voids, resulting bond/adhesion failure between coarse aggregate and
286 asphalt mastic. Similar observations were drawn previously by several researchers, concluding that adhesion failure is
287 the governing part in moisture damage [39,40].
288
289

290 **CONCLUSIONS**

291 The main conclusions from the research are;

- 292 • The influence of combined water and dynamic loading on asphalt surface damage was successfully simulated
293 in the laboratory environment. The test is simple to set-up, provides repeatable results, and capable of
294 assessing material performance with high frequency loading while the specimens are submerged in water.
295 The test has demonstrated promising future for further development as a screening test for water
296 susceptibility resistance of asphalt surfaces.
- 297 • In terms of mixture performance, depending on the type of asphalt surfaces, the presence of water and
298 continuous loading significantly accelerate surface cracking, rutting and ravelling.
- 299 • The cracking propensity was severe in highly open graded mixtures then the gap graded hot rolled asphalt.
300 Compared to dry condition testing, the appearance of surface crack was approximately seven times faster in
301 porous asphalt tested in wet conditions. It is interesting to note that while porous asphalt is designed to drain
302 water through open voids, the constant presence of water on the surface combined with loading can
303 significantly diminish their load-bearing capacity. It is therefore essential proper drainage for adequate
304 performance of open graded mixtures minimising the possibility of pore water build up in the clogged voids.
- 305 • As expected, all tested SMA mixtures demonstrated good rutting resistance compared to porous and hot
306 rolled mixtures, although their cracking resistance was significantly reduced in the presence of water.
- 307 • While both 10mm and 14mm HRA showed the best performance concerning resistance to cracking, the
308 rutting was significantly higher compared to other two mixtures. However, at the end of 40,000 pulses, the
309 porous asphalt showed significant rutting. The best performance was observed in 10mm SMA. The mixture
310 gradation appeared to have more influence on load-bearing capacity than the size of aggregates.
- 311 • Interesting to note that air voids do not seem to influence wet condition performance. For example, despite
312 similar void contents in SMA 14 and SMA 10, SMA 10 was not very sensitive to wet conditions as it was in
313 SMA14. It has appeared that aggregate nominal size may have an impact on wet condition performance.
314

315
316
317
318
319
320
321
322
323
324
325
326
327
328
329
330
331
332
333
334
335
336
337
338
339
340
341
342
343
344
345
346
347
348
349
350
351
352
353
354
355
356
357
358
359
360
361
362
363
364
365
366
367
368
369
370
371
372

REFERENCES

1. Gordon D. Aireya , Young-Kyu Choia. State of the Art Report on Moisture Sensitivity Test Methods for Bituminous Pavement Materials. , Vol. 3, No. 4, 2002, pp. 355-372.
2. Lottman, R. P. Laboratory Test Methods for Predicting Moisture-Induced Damage to Asphalt Concrete. , 1982.
3. Dehnad, M. H., A. Khodaii, and F. Moghadas Nejad. Moisture Sensitivity of Asphalt Mixtures Under Different Load Frequencies and Temperatures. Construction and Building Materials, Vol. 48, No. 0, 2013, pp. 700-707.
4. Cook, M., and P. E. S. Dynkins. Treated Permeable Base Offers Drainage, Stability. , May,1991.
5. Moulton, L. K. Highway Subdrainage Design, 1980.
6. Flynn, L. Open-Graded Base may Lengthen Pavement Life. Roads and Bridges, 1991, pp. 35-42.
7. Shiwakoti, H. Development of a Rapid Test to Determine Moisture Sensitivity of HMA [Superpave] Mixtures. ProQuest, 2007.
8. Little, D. N., and D. Jones. Chemical and Mechanical Processes of Moisture Damage in Hot-Mix Asphalt Pavements. In National Seminar on Moisture Sensitivity of Asphalt Pavements, 2003, pp. 37-70.
9. Saeed, F., S. Qamariatul, M. Rahman, and A. Woodside. The State of Pothole Management in UK Local Authority. Bituminous Mixtures and Pavements VI, 2015, pp. 153-159.
10. Alliance, A. I. Annual Local Authority Road Maintenance Survey. Asphalt Industry Alliance, London, UK, 2011.
11. Santucci, L. Moisture Sensitivity of Asphalt Pavements. Tech Topics, 2002.
12. Copeland, A., J. Youtcheff, and A. Shenoy. Moisture Sensitivity of Modified Asphalt Binders: Factors Influencing Bond Strength. Transportation Research Record: Journal of the Transportation Research Board, 2007.
13. Ahmad, N. Asphalt Mixture Moisture Sensitivity Evaluation using Surface Energy Parameters. , 2011.
14. Lindly, J. K., and A. S. Elsayed. Estimating Permeability of Asphalt-Treated Bases. Transportation Research Record, No. 1504, 1995, pp. 103-111.
15. Karlson, T. K. Evaluation of Cyclic Pore Pressure Induced Moisture Damage in Asphalt Pavement. University of Florida, 2005.
16. Kim, Y., J. S. Lutfi, A. Bhasin, and D. N. Little. Evaluation of Moisture Damage Mechanisms and Effects of Hydrated Lime in Asphalt Mixtures through Measurements of Mixture Component Properties and Performance Testing. Journal of Materials in Civil Engineering, Vol. 20, No. 10, 2008, pp. 659-667.
17. Willway, T., L. Baldachin, S. Reeves, and M. Harding. The Effects of Climate Change on Highway Pavements and how to Minimise them: Technical Report. The Effects of Climate Change on Highway Pavements and how to Minimise them: Technical Report, Vol. 1, No. 1, 2008, pp. 1-111.
18. Saeed, F., M. Rahman, and D. and Chamberlain. Impact of Tire and Traffic Parameters on Water Pressure in Pavement. Journal of Transportation Engineering, Part B: Pavements [ASCE]., 2018.
19. Masad, E., Birgisson, B., Al-Omari, A., Cooley, A. Analytical Derivation of Permeability and Numerical Simulation of Fluid Flow in Hot-Mix Asphalt. Journal of Materials in Civil Engineering, Vol. 16, No. 5, 2004, pp. 487-496.
20. Moghaddam, T. B., M. R. Karim, and M. Abdelaziz. A Review on Fatigue and Rutting Performance of Asphalt Mixes. Scientific Research and Essays, Vol. 6, No. 4, 2011, pp. 670-682.
21. Uhlmeyer, J., K. Willoughby, L. Pierce, and J. Mahoney. Top-Down Cracking in Washington State Asphalt Concrete Wearing Courses. Transportation Research Record: Journal of the Transportation Research Board, No. 1730, 2000, pp. 110-116.
22. Yu, B., Q. Lu, and J. Yang. Evaluation of Anti-Reflective Cracking Measures by Laboratory Test. International Journal of Pavement Engineering, Vol. 14, No. 6, 2013, pp. 553-560.
23. Abo-Qudais, S., and I. Shatnawi. Prediction of Bituminous Mixture Fatigue Life Based on Accumulated Strain. Construction and Building Materials, Vol. 21, No. 6, 2007, pp. 1370-1376.
24. Wen, H. Fatigue Performance Evaluation of WesTrack Asphalt Mixtures Based on Viscoelastic Analysis of Indirect Tensile Test. , 2001.
25. Myers, L. A., R. Roque, and B. E. Ruth. Mechanisms of Surface-Initiated Longitudinal Wheel Path Cracks in High-Type Bituminous Pavements. Journal of the Association of Asphalt Paving Technologists, Vol. 67, 1998.
26. Himeno, K., T. Kamijima, T. Ikeda, and T. Abe. Distribution of Tire Contact Pressure of Vehicles and its Influence on Pavement Distress. In Eighth International Conference on Asphalt Pavements Federal Highway Administration, 1997.
27. Nicholls, J., I. Carswell, C. Thomas, and B. Sexton. Durability of Thin Surfacing Systems. Part 4: Final

373 Report After Nine Years Monitoring. , 2010.
374 28. British Standards Institution.,. Bituminous Mixtures. Material Specifications. Hot Rolled Asphalt. British
375 Standards Institution, London, 2016.
376 29. British Standards Institution. Bituminous Mixtures Test Methods for Hot Mix Asphalt : Laboratory Mixing.
377 BS EN 12697-35, British Standards Institution, London, 2004.
378 30. Georgiou, P., and A. Loizos. A Laboratory Compaction Approach to Characterize Asphalt Pavement Surface
379 Friction Performance. *Wear*, Vol. 311, No. 1, 2014, pp. 114-122.
380 31. British Standards Institution. Test Methods for Hot Mix Asphalt. Determination of Bulk Density of
381 Bituminous Specimens. BS EN 12697-6, British Standards Institution, London, 2003.
382 32. Bituminous Mixtures. Test Methods for Hot Mix Asphalt. Determination of Void Characteristics of
383 Bituminous Specimens. BS EN 12697-8, British Standards Institution, London, 2003.
384 33. USM. The Engineering Properties and Performance of Porous Asphalt.
385 <https://www.google.co.uk/search?hl=en&q=www.civil.eng.usm.my/projekta/template/Chapter4.doc>,
386 Accessed 05/30, 2018.
387 34. Liu, H., P. Hao, and J. Xu. Effects of Nominal Maximum Aggregate Size on the Performance of Stone Matrix
388 Asphalt. *Applied Sciences*, Vol. 7, No. 2, 2017, pp. 126.
389 35. Rahman, M. and Thom, N. Performance of Asphalt Patch Repairs. *ice*, Institution of Civil Engineers, 2012.
390 36. Saeed, F. Measure Pore Water Pressure in Pavement. First year, Brunel University, London, 2015.
391 37. Saeed, F., Rahman, M. and Chamberlain, D. and [2018] 'A Novel Laboratory Test Method to Measure
392 Dynamic Water Pressure Underneath a Cracked Concrete Pavement', .
393 38. Miller, J. S., and W. Y. Bellinger. Distress Identification Manual for the Long-Term Pavement Performance
394 Program, 2003.
395 39. Apeagyei, A. K., J. R. Grenfell, and G. D. Airey. Influence of Aggregate Absorption and Diffusion Properties
396 on Moisture Damage in Asphalt Mixtures. *Road Materials and Pavement Design*, Vol. 16, No. sup1, 2015,
397 pp. 404-422.
398 40. Nguyen, T., E. Byrd, D. Alsheh, and D. Bentz. Relation between Adhesion Loss and Water at the
399 polymer/substrate Interface. In *Proceedings Adhesion Society Meeting*, Hilton Head Island, SC, 1995.

400
401
402
403
404
405
406
407
408